AI-Enhanced UWB–Cartographer SLAM for Drift-Accumulating Indoor Environments

Oyasi Zaki Ananta
Dept. of Information and Communication Engineering
Chosun University
Gwangju, South Korea
oyasi@chosun.ac.kr

Dae-Ho Kim
Dept. of Artificial Intelligence Engineering
Chosun University
Gwangju, South Korea
wireless@chosun.ac.kr

Jae-Young Pyun*
Dept. of Information and Communication Engineering
Chosun University
Gwangju, South Korea
jypyun@chosun.ac.kr

***Abstract*—In simultaneous localization and mapping (SLAM), accumulated drift error caused by odometry noise and inefficient loop closure detection is inevitable limitation for frameworks such as 2D Cartographer. In recent studies researchers have introduced ultra-wideband (UWB) to Cartographer and other SLAM frameworks to alleviate drift accumulation issue, when using a dense UWB anchor deployment. However, this UWB infrastructure could be unsuitable for large facilities like long corridors and industrial plants where the drift occurs most. In response to such an issue, this paper proposes a resource-efficient localization framework that tightly couples UWB ranging with Cartographer through a zone-based single anchor deployment using an AI-enhanced drift control strategy. The proposed system employs a hierarchical processing chain consisting of signal validation, Kalman filtering, exponential smoothing, and two additional components: a Smart Anomaly Detector for adaptive confidence assignment and a Drift Predictor for boosting AI correction. Experiments conducted on a trajectory of approximately 144 m trajectory demonstrate an 85.50% reduction in mean drift and an 84.82% improvement in RMSE relative to the pure Cartographer, along with a 52.37% performance gain over the pure UWB-Cartographer fusion.**

***Index Terms*—Ultra-wideband (UWB), Cartographer, SLAM, sensor fusion, indoor localization, anomaly detection.**

I. Introduction

Indoor mobile robot operating strictly depends on the SLAM for enabling autonomous navigation, mapping, and situational awareness. Google Cartographer has proven to be one of the most popular SLAM frameworks for 2D LiDAR-based mapping in real-time [1]. However, due to wheel slippage, sensor noise, and a lack of loop-closure chances, Cartographer and other odometry-driven SLAM systems suffer from cumulative longitudinal drift in long corridor-like environments and large open facilities [2], [3]. This drift increases uncontrollably over long trajectories in the absence of trustworthy external references, reducing map consistency and localization accuracy.

Because of its excellent multipath resilience, durability under non-line-of-sight situations, accurate time-of-flight ranging and ultra-wideband (UWB) localization has been thoroughly studied as an external absolute location reference for indoor robotics [4], [5]. Previous UWB-assisted SLAM techniques that integrate range-based constraints into pose-graph optimization have shown significant drift reduction [6], [7]. Nevertheless, the majority of current systems depend on dense anchor installations to guarantee favorable geometric observability and continuous coverage [8], [9]. Particularly in large-scale settings like industrial buildings, warehouses, extensive corridors and dense infrastructure greatly raises hardware costs, installation effort, calibration complexity and long-term maintenance strain [10].

Odometry, LiDAR, inertial sensors, and external positioning systems have all been included in recent multi-sensor fusion studies to increase SLAM robustness [11]–[13]. Although most of these methods improve performance, they are limited in their capacity to adjust to changing motion dynamics, signal quality and environmental variables since they rely on static confidence assumptions and fixed fusion parameters [14]. Furthermore, few current frameworks specifically address how to decrease UWB hardware deployment burden across long, open-loop trajectories while maintaining robust drift-bounding capacity [15].

In order to overcome these difficulties, this study suggests a resource-efficient UWB–SLAM fusion framework that tightly integrates UWB ranging with 2D Cartographer using AI-enhanced drift control and a zone-based single-anchor technique. The environment is divided into longitudinal zones, where only one anchor is actively fused at a time, rather than requiring extensive anchor coverage. This solution preserves enough geometric constraints to limit drift while significantly lowering deployment costs and infrastructure complexity. The proposed architecture uses two lightweight AI components, in contrast to traditional fixed-gain fusion techniques: (i) a Smart Anomaly Detector that uses statistical consistency, rate-of-change behavior, and short-term stability to assign adaptive confidence scores to UWB measurements, and (ii) a lightweight Long Short-Term Memory (LSTM) network that uses temporal sensor patterns to determine the best fusion weights. The LSTM, with two hidden layers of 32 and 16 units (about 1,500 trainable parameters), continually adjusts to drift velocity, signal quality, and motion dynamics throughout a 10-timestep prediction window by learning from data to forecast when and how strongly to apply UWB adjustments.

*Corresponding author: Jae-Young Pyun (email: jypyun@chosun.ac.kr)

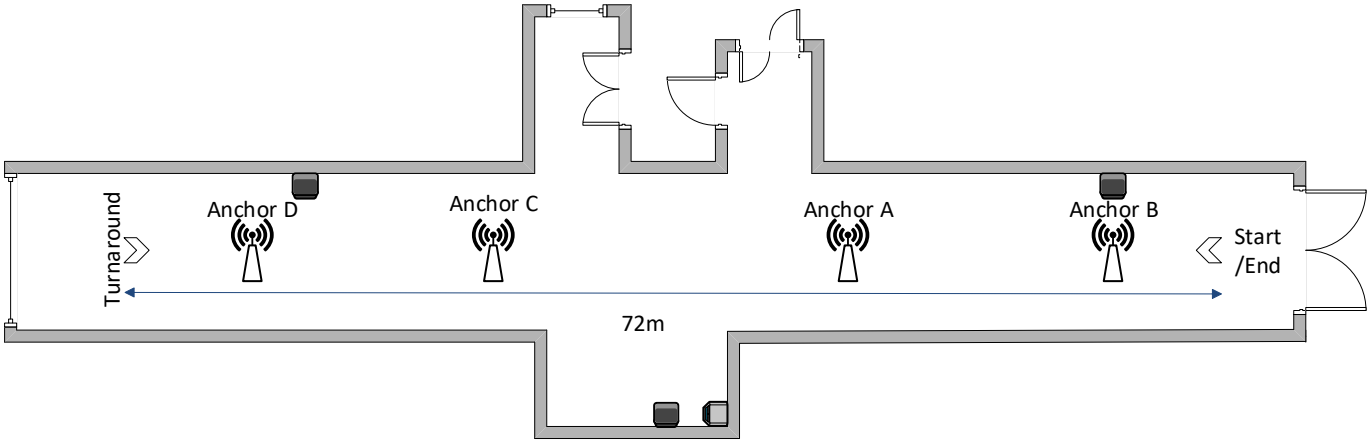

Fig. 1: Long corridor floor plan.

This work proposes a zone-based UWB–Cartographer fusion framework with the following key contributions:

1) *Zone-Based Anchor Selection:* In order to minimize infrastructure costs, only one anchor is selected based on longitudinal position that is active at any given moment.
2) *AI-Enhanced Processing:* A Smart Anomaly Detector provides context-aware confidence scores while a Drift Predictor performs proactive drift control.
3) *Authority Architecture:* UWB functions as a bounded soft constraint, while Cartographer's transform is absolute for both pose and direction.
4) *Proven Performance:* Up to 85.50% drift reduction and 84.82% RMSE improvement over pure Cartographer.

II. Related Work

For indoor mobile robots, many SLAM and fusion frameworks have been developed, especially in GNSS-denied environments. For portable indoor mapping and tracking, Nguyen *et al.* thoroughly assessed a number of ROS-based 2D LiDAR SLAM algorithms, such as Cartographer, Gmapping, and Hector SLAM [16]. Their findings demonstrate that Cartographer provides good real-time performance and mapping quality, but they also show that scene geometry and loop-closure opportunities have a significant impact on performance, which highlights the necessity for extra absolute references in long, feature-sparse settings.

UWB is frequently combined with LiDAR in tightly connected frameworks and has been extensively investigated as such an external reference. Liu et al. suggested a low-cost mapping system that uses graph optimization to combine UWB and short-range 2D LiDAR, where LiDAR loop closure refines the map and UWB anchors offer global constraints [17]. Although their method relies on several anchors and does not specifically target lengthy corridor-like trajectories, it focuses on lowering hardware costs without sacrificing mapping accuracy. In order to reject poor UWB data, Chen et al. introduced an enhanced closely connected UWB/LiDAR-SLAM system with non-line-of-sight (NLOS) identification using LiDAR point clouds [18]. Although they showed notable improvements in positioning accuracy in GNSS-denied environments, the focus is on dense infrastructure and NLOS handling instead of reducing the number of anchors over long open-loop courses.

UWB-LiDAR fusion has been used for high-precision object tracking in addition to robot localization. Li *et al.* presented LUGOT, a LiDAR–UWB object-tracking framework that uses a customized fusion technique to jointly exploit LiDAR point clouds and UWB ranging to achieve centimeter-level precision and zero ID switches [19]. LUGOT shows the potential of UWB–LiDAR fusion to deliver reliable, high-accuracy spatial awareness in congested interior situations, despite focusing on moving-object tracking rather than robot position estimation.

Instead of using dense multi-anchor coverage or only NLOS-focused filtering, our method specifically focuses on long and featureless corridor navigation with 2D Cartographer and aims to reduce UWB infrastructure by using a zone-based single-anchor strategy along with AI-enhanced, context-aware weighting of UWB constraints.

III. System Architecture

A. Experimental Environment

All experiments carried out in a straight indoor hallway runway that was roughly 72 m long overall. The robot travels a complete out-and-back trajectory, including a turnaround area at the far end of the corridor, beginning and ending at the same spot (Start/End point). The corridor is a difficult environment for pure LiDAR-based Cartographer since it is primarily feature-sparse over its length, with parallel walls and few unique geometric landmarks.

As shown in Fig. 1, four UWB anchors (A, B, C, and D) are placed along the corridor in fixed locations within the global map frame. The corridor is roughly divided into longitudinal segments by the placement of anchors: Anchor B in the start region, Anchor A in the first middle segment, Anchor C toward the far middle segment, and Anchor D near the turnaround area. Using the zone-based single-anchor

strategy, only one anchor is actively fused at a time based on the robot's longitudinal location.

B. Hardware Architecture

The proposed system is implemented on ROS2 (Robot Operating System 2), and the hardware architecture of the system is structured as shown in Fig. 2.

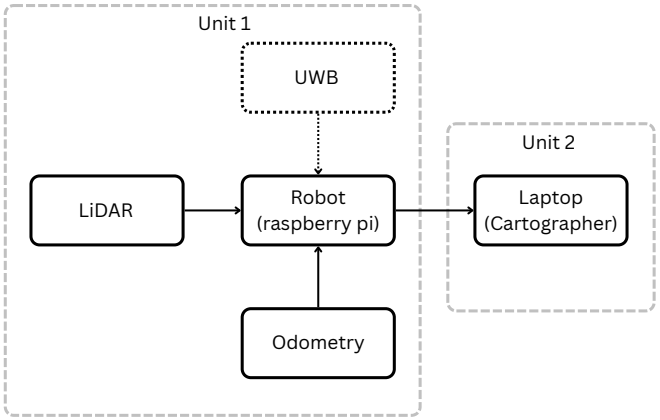

Fig. 2: Hardware architecture of the robot system

The proposed UWB-Cartographer robot system has been implemented with two different units. One of them is the raspberry pi 4 which is connected to all the sensors (LiDAR, Odometry and UWB). Another unit (Laptop) is responsible for running Cartographer and visualizing the map building and navigation through Rviz.

C. Software Architecture

The proposed UWB-Cartographer robot system architecture consists of a tightly coupled UWB-Cartographer fusion node that runs in mobile robot equipped with a UWB tag, LiDAR, and wheel odometry. The node receives two main input streams: (i) raw UWB distances from multiple anchors deployed along the corridor, and (ii) the map to base_link transform from Cartographer, which provides the current robot pose at 20 Hz. At startup, the fusion node loads the fixed positions of all UWB anchors in the global map frame and initializes per-anchor filtering states.

On the UWB side, raw distance measurements from the currently active anchor pass through a hierarchical preprocessing pipeline. First, a range validation stage removes physically implausible measurements based on the minimum and maximum distance defined in the anchors' position and range setup in the UWB-Cartographer node package. The remaining samples are filtered by a scalar Kalman filter to suppress noise and spikes, followed by exponential smoothing that enforces temporal consistency in the distance signal. In order to determine confidence scores [20], the Smart Anomaly Detector is applied to assess the measurements' statistical consistency, short-term stability, and rate of change. The resulting pair is stored in an internal processed UWB data buffer associated with the corresponding anchor.

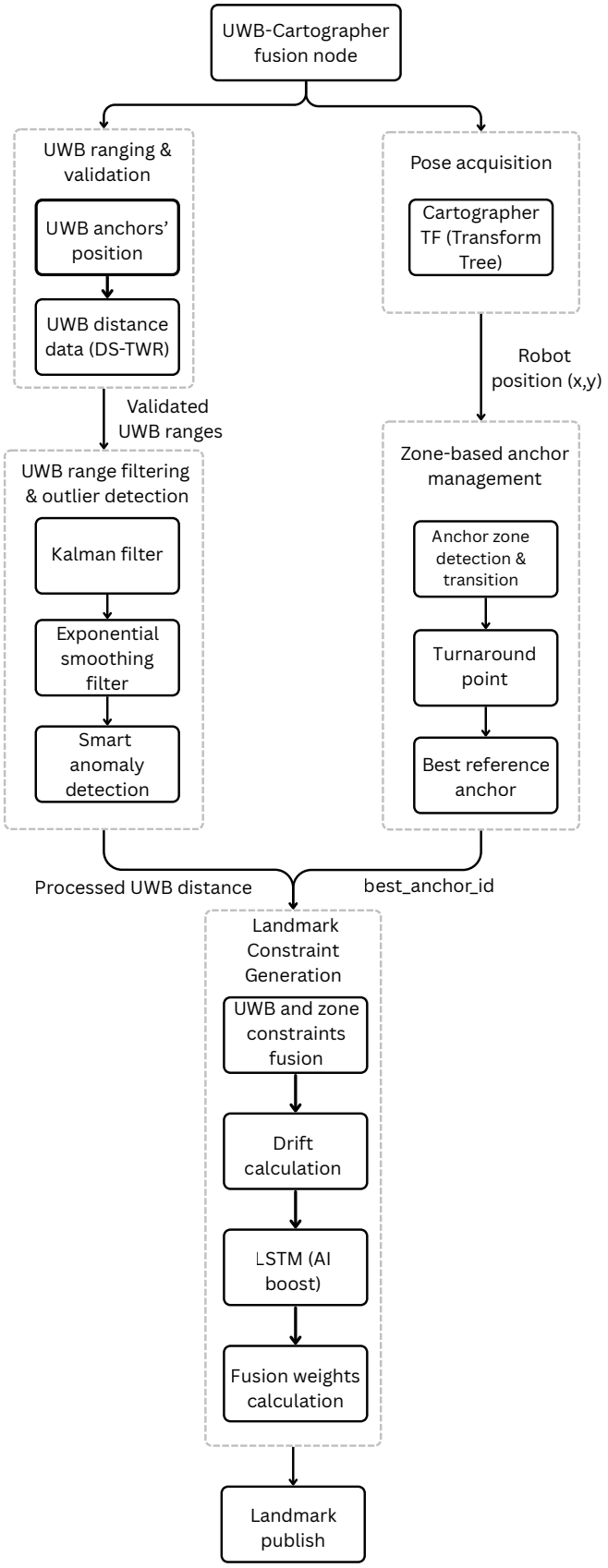

Fig. 3: Software architecture of the proposed AI based UWB–Cartographer fusion pipeline.

For diagnostic and zone selection purposes, the node continuously accesses Cartographer's TF (Transform Tree) to determine the robot's present position. The odometry system publishes odom to base_link (raw wheel encoder data), the cartographer publishes map to odom (drift-corrected global frame), and TF automatically combines them to generate map to base_link, which gives the robot's current posture estimate. Crucially, the fusion node only uses the TF position for zone identification and drift computation; it never directly affects this posture. The zone detection function uses the TF pose to determine the active longitudinal zone based on the robot's x-coordinate. It also applies special handling for turnaround regions (extended zones at path endpoints) and verifies zone transitions in accordance with sequential path constraints (for bidirectional travel between anchors). The optimal anchor for the current zone is then chosen by the node, provided that the zone-appropriate anchor has current, correct data. The node ensures safe degradation to TF-only operation by publishing an empty landmark list instead of using faulty data if the necessary anchor is unavailable or its data is stale .

The node uses a multi-stage pipeline to process raw UWB distance measurements for valid anchors: range validation filters physically impossible readings, a Kalman filter eliminates transient spikes, exponential smoothing lowers high-frequency noise and a Smart Anomaly Detector assigns confidence scores based on rate-of-change analysis and statistical consistency. The geometric drift is the difference between the robot's TF position and the position suggested by the UWB distance circle around the anchor's known location that can be calculated using this processed distance in conjunction with the TF pose. The main novelty of this approach is that drift modifies landmark trust rather than immediately correcting position. Drift lowers landmark weight in baseline mode (low trust if high drift). The LSTM Drift Predictor generates an adaptive gain factor ai_boost in AI mode by analyzing drift history, drift velocity, robot speed, and context (such as turnaround vs. straight course). In situations where high drift reflects TF error rather than UWB error (such as wheel slide during turnarounds), the LSTM suitably increases correction strength and, on the other hand, decreases weight during transient spikes (such as anchor swaps).

A base scaling factor (increased during turnarounds), the Smart Anomaly Detector's confidence score, drift-based adjustment (1.0 - drift/5m), distance-dependent attenuation (1.0 - distance/20m), transition smoothing (ramped over 10 cycles during anchor switches), and the AI-derived ai_boost (0.3–2.0×) are all included in the final landmark weight. This weight and the fixed world-frame position of the anchor constitute a landmark constraint that is submitted to Cartographer using the /landmark topic. The actual fusion is then carried out by Cartographer's pose-graph optimizer, which treats the TF estimate (via wheel odometry and scan matching) and the UWB landmark constraint (anchor position + measured distance + weight) as distinct observations of the robot's pose. Higher landmark weights bring the solution closer to the UWB-implied position when the optimizer uses weighted least-squares minimization to combine these inputs. Because Cartographer's optimizer automatically resolves conflicts between odometry, scan matching and UWB constraints based on their relative weights and spatial consistency, this method guarantees smooth, globally-consistent fusion without position discontinuities.

In particular, during long, open-loop corridor lengths where wheel odometry accumulates error and scan matching offers little correction, the outcome is an updated robot trajectory and map with dramatically decreased drift. The technique achieves robust drift correction while preserving stability during transient anomalies by adaptively weighting UWB landmarks based on learnt drift patterns instead of directly overriding TF placements.

D. Zone-Based Anchor Selection

The environment is partitioned into four longitudinal zones which is defined on the base of anchors. Each anchor's zone is defined by the anchor's name itself. For example, Zone B is within 18m range from the anchor's position in the world map. Same method is applied to fix Anchor A, C and D's zone too. This method of binding the range with anchors' position favors choosing data from nearest anchor instead of some random anchor. Zones for the anchors are:

1) *Zone B:* $x < 18\,\text{m}$ (near turnaround)
2) *Zone A:* $18\,\text{m} \leq x < 36\,\text{m}$
3) *Zone C:* $36\,\text{m} \leq x < 54\,\text{m}$
4) *Zone D:* $54\,\text{m} \leq x$, (far turnaround)

Zone boundary oscillation is prevented with a 20-cycle cooldown (sim1s at 20Hz) between anchor transitions, which is cut in half for responsiveness during turnarounds.

E. Authoritative Pose and Drift

Cartographer's transform is the authoritative pose estimate at all times:

$$P_{\text{robot}} = P_{\text{carto}} = P_(x_{\text{carto}}, y_{\text{carto}}), \tag{1}$$

where x_{carto} and y_{carto} are the Cartesian coordinates that we get from the Cartographer's TF data. Then we use them as robot's coordinates.
The disagreement between Cartographer and UWB is quantified as a scalar drift:

$$\text{drift} = \left\| P_{\text{carto}} - P_{\text{uwb}} \right\|, \tag{2}$$

where P_{uwb} is the UWB-implied robot position obtained by projecting the smoothed UWB range along the line from the anchor to P_{carto}. Intuitively, drift measures how far the SLAM estimate has deviated from the external UWB reference. Large values indicate that Cartographer has accumulated significant error along the trajectory.

F. Drift Predictor

To react not only to the current drift but also to its trend, a drift velocity is estimated over a sliding time window:

$$v_{\text{drift}} = \frac{\text{drift}_t - \text{drift}_{t-N}}{t - t_N}, \tag{3}$$

where drift_t is the current drift at time t, drift_{t-N} is the drift N samples earlier, and t_N is the corresponding timestamp. The parameter N controls the temporal horizon over which the change is evaluated. A positive v_{drift} indicates that drift is growing over time (the SLAM estimate is gradually diverging from UWB), whereas a negative v_{drift} indicates that drift is being reduced. This quantity is used by our AI model to decide when to strengthen or weaken the contribution of UWB landmarks in the pose graph.

G. Landmark Weight

Each UWB measurement is converted into a landmark constraint with an adaptive weight

$$w = w_{\text{base}} \cdot c \cdot w_{\text{distance}} \cdot w_{\text{transition}} \cdot \dot{a}i_{\text{boost}}, \tag{4}$$

here w_{base} is a global scaling factor that sets the overall importance of UWB constraints relative to LiDAR and odometry. The term $c \in [0.7, 1.0]$ is a confidence score produced by the Smart Anomaly Detector. It decreases when the UWB signal appears noisy, inconsistent, or unstable, and remains close to 1.0 for clean and reliable measurements. The factor w_{distance} implements distance-dependent attenuation, so that anchors exert weaker influence when the robot is far away, which reduces over-constraining effects in distant regions. The factor $w_{\text{transition}}$ modulates the weight during zone transitions, damping the impact of UWB when the active anchor changes in order to avoid sudden jumps at zone boundaries. Finally, $\text{ai}_{\text{boost}} \in [0.3, 2.0]$ is an adaptive correction factor predicted by a two-layer LSTM network trained on expert demonstration data. The LSTM receives 10-timestep sequences of four UWB distance features, confidence score, geometric drift (TF-UWB position discrepancy) and drift velocity from which it learns context-dependent correction strategies. The network boosts weights to 1.8–2.0× when high drift coincides with wheel slip conditions (turnarounds, low speed), suppresses to 0.3–0.5× during transient spikes from anchor switches, and maintains 1.0× during stable operation. This temporal pattern recognition enables proactive drift correction based on learned scenarios rather than reactive threshold rules, with the output clipped to ensure pose-graph optimization stability.

IV. Results Analysis

A. Performance Comparison

In this study, we evaluate three variants of the SLAM system: (1) the pure Cartographer (Baseline), (2) Cartographer enhanced with UWB sensor fusion (UWB-Enhanced), and (3) our proposed Cartographer-UWB system with AI-driven drift correction (Proposed).

TABLE I: Performance Comparison (in meters)

Metric	Baseline	UWB-Enhanced	Proposed
Mean Drift	4.15	1.26	0.60
Std Dev	2.84	1.60	0.47
Max Drift	10.36	6.11	2.31
RMSE	5.03	2.05	0.76

For safe navigation and precise mapping in our indoor corridor environment, we consider a mean position drift of less than 1.0 m to be acceptable. Our test corridor is 2.54 m wide, so keeping mean localization drift below 1.0 m ensures the robot remains within the corridor and preserves sufficient lateral clearance to both walls for safe navigation and docking in our setup. Under this criterion, the Proposed fusion (mean drift 0.60 m, max drift 2.31 m) is acceptable, whereas the Baseline configuration (mean drift 4.15 m) is not.

B. Aggregate Metrics and Improvements

Key improvements are:

1) *UWB-Enhanced vs. Baseline:* 69.56% mean drift reduction.
2) *Proposed vs. UWB-Enhanced:* 85.50% mean drift and 85.88% RMSE reduction.
3) *Proposed vs. UWB-Enhanced:* 52.37% additional mean drift reduction.

C. Drift comparison

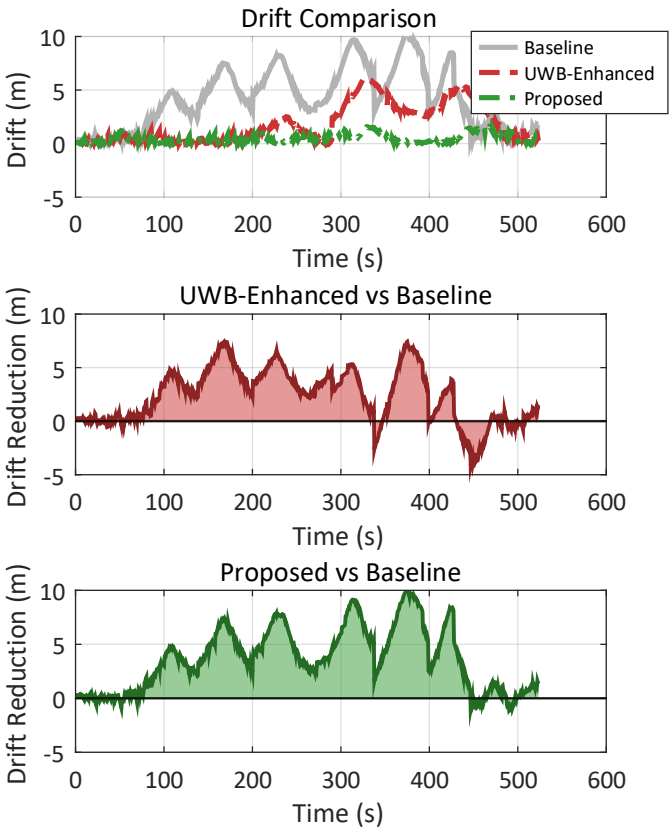

Fig. 4: Drift comparison overtime. Top: direct drift comparison over time for all three configurations. Middle: drift reduction of UWB-Enhanced relative to Baseline (positive is better). Bottom: drift reduction of Proposed relative to Baseline.

Drift over time for Cartographer without UWB, the basic UWB–Cartographer fusion, and the proposed AI-based fusion are compared in Fig. 4. The top plot demonstrates that the baseline fusion substantially mitigates these errors, while the

"Baseline" case accumulates huge drift peaks above 9 m. For nearly the whole run, the Proposed approach keeps drift at minimal levels. Drift reduction in comparison to the "Baseline" is expressed in the lower subplots, showing that the Proposed fusion routinely produces positive and significantly greater reductions than the Baseline.

D. Map comparison

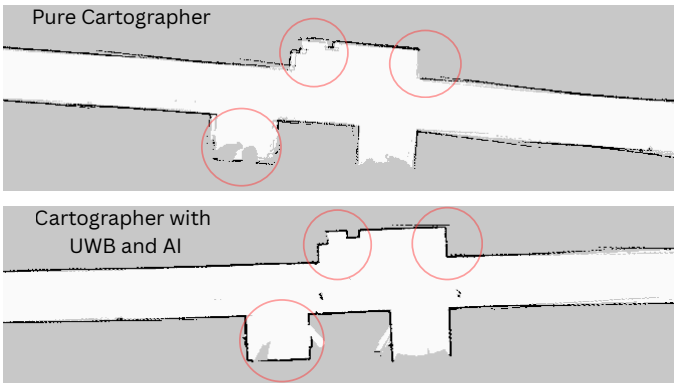

Fig. 5: Map generated in the proposed robot system without and with UWB and AI.

The map in Fig. 5 was generated in the environment shown in Fig. 1 using Cartographer and visualized in Rviz. In Fig. 5 we can see the difference between pure Cartographer and Cartographer with UWB and AI generated map, which proves that drift reduction also affects the map generation as our system is capable of correcting drift accumulation in real time. This ultimately improves the map quality by reducing overlapped issue and generates clearer map.

V. Conclusion

This research developed a resource-efficient UWB–SLAM fusion system that uses a lightweight AI model and a zone-based single-anchor method to tightly integrate UWB range with 2D Cartographer. The UWB-Enhanced method decreases mean drift from 4.15 m to 1.26 m (a 69.56% improvement) and RMSE from 5.03 m to 2.04 m (an 80.18% improvement) when compared to pure Cartographer, according to experiments conducted in a 72 m feature-sparse corridor. In addition to lowering drift standard deviation by 83.45%, the proposed system also reduces mean drift to 0.60 m and RMSE to 0.76 m, which represent gains over the baseline of 85.50% and 84.82%, respectively. These findings demonstrate that zone-based single-anchor deployment, in conjunction with drift prediction and adaptive anomaly detection, may successfully constrain longitudinal drift in the absence of dense UWB infrastructure, enhancing long-corridor SLAM accuracy and consistency.

VI. Acknowledgement

This research was supported by the BrainKorea21Four Program through the National Research Foundation of Korea (NRF) funded by the Ministry of Education (4299990114316).

References

[1] W. Hess, D. Kohler, H. Rapp, and D. Andor, "Real-time loop closure in 2D LIDAR SLAM," in *IEEE Int. Conf. Robot. Autom. (ICRA)*, 2016, pp. 1271–1278.
[2] K. Trejos, J. C. G. Pimentel, and M. Teran, 2D SLAM algorithms characterization, calibration, and comparison considering loop closure," *Sensors*, vol. 22, no. 18, pp. 7034, 2022.
[3] L. Jiang and M. Zhang, An improved laser SLAM algorithm based on Cartographer," in *Int. Conf. Artif. Life Robot. (ICAROB)*, 2025, pp. 104–107.
[4] S. Gezici *et al.*, "Localization via ultra-wideband radios: a look at positioning aspects for future sensor networks," *IEEE Signal Process. Mag.*, vol. 22, no. 4, pp. 70–84, 2005.
[5] N. Xu *et al.*, A survey on ultra wide band based localization for mobile autonomous machines," *Robot. Auton. Syst.*, vol. 175, pp. 104658, 2025.
[6] Y. Song *et al.*, UWB/LiDAR fusion for cooperative range-only SLAM," *arXiv preprint arXiv:1811.02854*, 2019.
[7] J. Wang, T. Zhang, and Y. Jin, Research on mobile robot localization and mapping based on UWB/LiDAR fusion," *IEEE Access*, vol. 9, pp. 12345–12356, 2021.
[8] R. Garg *et al.*, "Large network UWB localization: Algorithms and system design," in *Proc. USENIX Symp. Netw. Syst. Design Impl. (NSDI)*, 2025.
[9] B. Van Herbruggen *et al.*, Multihop self-calibration algorithm for ultra-wideband localization," *IEEE Internet Things J.*, vol. 10, no. 14, pp. 12345–12356, 2023.
[10] J. Cho *et al.*, A study on anchor placement and 3D positioning accuracy in construction sites," *Autom. Constr.*, vol. 158, pp. 105185, 2024.
[11] R. C. Luo *et al.*, A review of multi-sensor fusion SLAM systems based on 3D LiDAR," *Remote Sens.*, vol. 14, no. 12, pp. 2835, 2022.
[12] D. Zhang *et al.*, Towards robust sensor-fusion ground SLAM: A benchmark and resilient framework," *arXiv preprint arXiv:2507.08364*, 2025.
[13] Y. Cai *et al.*, A comprehensive review on multi-sensor fusion and SLAM for autonomous driving," *Int. J. Semantic Web Inf. Syst.*, vol. 19, no. 1, 2023.
[14] Z. Lin *et al.*, Research on SLAM algorithm based on multisensor fusion for complex environments," in *Proc. SPIE*, vol. 13965, 2025, Art. no. 139650B.
[15] R. A. Deshmukh *et al.*, "Advancing indoor positioning systems: Innovations, challenges, and applications," *Robotica*, vol. 43, no. 2, pp. 1–25, 2025.
[16] Q. H. Nguyen, P. Johnson, and D. Latham, "Performance evaluation of ROS-based SLAM algorithms for handheld indoor mapping and tracking systems," *IEEE Sensors J.*, vol. 23, no. 1, pp. 706–714, Jan. 2023.
[17] R. Liu *et al.*, "Cost-effective mapping of mobile robot based on the fusion of UWB and short-range 2-D LiDAR," *IEEE/ASME Trans. Mechatronics*, vol. 27, no. 3, pp. 1321–1331, Jun. 2022.
[18] Z. Chen *et al.*, "Improved-UWB/LiDAR-SLAM tightly coupled positioning system with NLOS identification using a LiDAR point cloud in GNSS-denied environments," *Remote Sens.*, vol. 14, no. 6, pp. 1380, 2022.
[19] Y. Li *et al.*, "LUGOT: LiDAR–UWB object tracking with zero ID switches and centimeter-level precision," *IEEE Internet Things J.*, vol. 12, no. 22, pp. 48945–48961, Nov. 2025.
[20] Q. Yuan, F. Yan, Z. Yin, C. Lv, J. Hu, Y. Li, and J. Wang, "An integrated LSTM-rule-based fusion method for the localization of intelligent vehicles in a complex environment," *Sensors*, vol. 24, no. 12, art. 4025, 2024, doi: 10.3390/s24124025.